Equilibrium and kinetics in the (111) surface of Cu-Ag alloys: Comparison between mean-field and Monte Carlo calculations

Andrés Saúl and Bernard Legrand
Section de Recherches de Métallurgie Physique/Département des études du Comportement des Matériaux, Centre d'Etudes Nucléaires de Saclay, C.E. Saclay, 91191 Gif-sur-Yvette Cedex, France

Guy Tréglia
Centre de Recherche sur les Mecanismes de la Croissance Cristalline-Centre National de la Recherche Scientifique, Campus de Luminy, Case 913, 13288 Marseille Cedex 9, France
(Received 3 February 1994)

In this paper we study the relationship between equilibrium and kinetics in Cu-Ag (111). We investigate the kinetics of segregation in a silver–dilute-copper sample and the dissolution kinetics of one Ag monolayer deposited on Cu(111). We compare results obtained using mean-field and Monte Carlo methods and relate them to the equilibrium isotherm by means of a local-equilibrium concept. We find good agreement with available experimental results on segregation kinetics and on dissolution kinetics when the Monte Carlo simulation is used.

I. INTRODUCTION

In bimetallic alloys A_cB_{1-c} the relative concentration of the alloy constituents near the surface is in general different than in the bulk giving rise to the surface segregation phenomena. For a given temperature the equilibrium surface concentration depends in general on the surface orientation, the size mismatch of the constituents, the difference in surface energies, and the type of chemical bonding of the atomic species. Many of these effects have been studied theoretically in metallic alloys.[1–5]

From the kinetic point of view, two kinds of studies are of interest: the kinetics of surface segregation, that is, how the equilibrium surface segregation is established from an initial nonequilibrium condition, and the kinetics of dissolution of one or several A monolayers that were initially deposited on a free B surface. The kinetics of surface segregation cannot be theoretically interpreted by means of the standard Fick's description of the flux of matter being proportional to the concentration gradient because it cannot explain uphill diffusion. On the other hand, during the kinetics of dissolution a metastable surface alloy can be formed in some cases. Moreover, when the surface energy of the deposit is higher than the substrate one a surfactant effect could happen.[6–8] It is necessary to have a theory that takes into account not only the surface energetic factors but also the tendency of the alloy to either form ordered phases or to phase separate. In this sense, different models have been proposed to study segregation kinetics near a solid surface that are consistent with the equilibrium surface segregation[9–13] and some of them also account for the bulk properties. These models are one-dimensional (1D) multilayer models that deal with homogeneous concentrations per plane parallel to the free surface. The in-plane inhomogeneity is not taken into account in these models and short and long distance in-plane ordering as well as correlations are neglected. To go beyond these limitations one could use more sophisticated mean-field models or Monte Carlo ones.

The equilibrium and kinetics on the (111) surface of Cu-Ag alloys have been studied experimentally[14–16] and theoretically.[17–19] Regarding the equilibrium properties and from the bulk point of view the Cu-Ag system is one with a tendency to phase separation and from the surface point of view it presents a strong tendency to silver segregation. It has also been shown that layering transitions occurs in the (111) surface of Cu-Ag (the near surface concentrations going from low to high silver concentration by lowering the temperature or increasing the bulk concentration).[14–20]

There have also been experimental studies of the kinetics of surface segregation and the kinetics of dissolution of one monolayer of Ag on Cu(111) using Auger spectroscopy.[16] They show a linear growth of the surface silver concentration with the square root of time in segregation kinetics and a linear decrease of the surface concentration with square root of time during dissolution.[21] During these kinetic studies the part of the surface phase diagram where the system undergoes the mentioned layering transition is explored. One can then wonder up to what extent these one-dimensional mean-field models are able to describe the experimental results. It was found that a mean-field model correctly describes the experimental result during segregation kinetics but not during the kinetics of dissolution.[22,23]

The aim of this paper is then to compare two different theoretical approaches: a simple one-dimensional mean-field model and a Monte Carlo model when applied to the segregation equilibrium and to the kinetics of segregation and dissolution in Cu-Ag alloys and also to compare them with available experimental data. Both models are based on the same effective tight binding Ising model[5,24] that takes into account the surface segregation parameters and the tendency of the bulk to phase separate or to form ordered phases. However, we are aware that both

models being rigid lattice ones do not take into account in a rigorous way the displacement of the atoms during the diffusion process that can be important due to the large size mismatch of about 12%.

II. THE NUMERICAL MODEL

It is well known that the total energy of transition metal alloys A_cB_{1-c}, where d electrons play a predominant role, cannot be written as a sum of pair interactions. Nevertheless it has been demonstrated that the part of the energy that depends on the actual configuration can be calculated as an Ising model with effective pair interactions. These effective pair interactions are calculated from the tight binding electronic structure of a totally disordered alloy in the coherent potential approximation.[25]

The generalization of this model to surfaces of transition metal alloys is the tight binding Ising model (TBIM).[5,24] The internal energy is then written

$$H^{\mathrm{TBIM}} = \sum_n p_n \left\{ \Delta h_n^{\mathrm{eff}} + \Delta H_n^{\mathrm{size}} - \sum_{m \neq n} V_{nm} \right\} + \sum_{n,m \neq n} p_n p_m V_{nm}, \quad (1)$$

where p_n is the spinlike occupation variable equal to 1 (0) if the site n is occupied by an atom A (B). Let us recall the main features of the model.

(i) V_{nm} is the effective pair interaction between atoms at sites n and m:

$$V_{nm} = \tfrac{1}{2}(V_{nm}^{\mathrm{AA}} + V_{nm}^{\mathrm{BB}} - 2V_{nm}^{\mathrm{AB}}), \quad (2)$$

for fcc systems it is negligible if n and m are not first neighbor sites. It takes a constant value $V_{nm} = V$ if n and m are bulk sites and characterizes the tendency to bulk ordering ($V > 0$) or to phase separation ($V < 0$). When at least one site belongs to the surface, the interaction V_{nm} is enhanced being $V_0 = 1.5V$ for the close packed (111) and (100) fcc surfaces and $V_0 = 2V$ for the (110) one.

(ii) The linear term $\Delta h_n^{\mathrm{eff}}$ is related to the difference in surface energies between the pure constituents, and is generally different from zero only for the surface and first underlayer planes.

(iii) $\Delta H_n^{\mathrm{size}}$ accounts for a possible size effect, this term is calculated by means of a tight binding quenched molecular dynamics[26–28] and is only significant close to the surface. In this scheme $\Delta H_n^{\mathrm{size}}$ is calculated as the size dependent part of the difference between the total energy when a single impurity is moved from the totally relaxed bulk to the totally relaxed surface. For a given bulk concentration this value decreases with the surface concentration c_0;[17] however, for simplicity in this work we have used a constant value calculated in the surface and bulk dilute case ($c_0, c \to 0$).

A. Mean-field statics

In this section we present the model used within the mean-field approximation. In this case, the relevant quantities are the concentration of A atoms in the i plane parallel to the surface c_i ($i = 0$ being the surface plane). This assumption of homogeneous concentration per plane gives rise to a one-dimensional model where the grand-canonical free energy is written

$$G = \langle H^{\mathrm{TBIM}} \rangle - T\langle S \rangle - \mu \langle N_A \rangle. \quad (3)$$

$\langle H^{\mathrm{TBIM}} \rangle$ represents the mean value of the internal energy calculated from Eq. (1):

$$\begin{aligned}\langle H^{\mathrm{TBIM}} \rangle = {} & c_0 N_p \{\Delta H_0^{\mathrm{size}} + \Delta h_0^{\mathrm{eff}} - V_0(Z+Z') + V_0(Zc_0 + Z'c_1)\} \\ & + c_1 N_p \{\Delta H_1^{\mathrm{size}} + \Delta h_1^{\mathrm{eff}} - V(Z+Z') - V_0 Z' + V(Zc_1 + Z'c_2) + V_0 Z' c_0\} \\ & + \sum_{i \geq 2} c_i N_p \{-V(Z+2Z') + V[Zc_i + Z'(c_{i+1} + c_{i-1})]\}. \end{aligned} \quad (4)$$

$\langle S \rangle$ is the mean value of the entropy:

$$\langle S \rangle = -kN_p \sum_{i=0}^{\infty} [c_i \ln(c_i) + (1-c_i)\ln(1-c_i)]. \quad (5)$$

$\langle N_A \rangle$ is the mean number of A atoms in the system:

$$\langle N_A \rangle = N_p \sum_{i=0}^{\infty} c_i. \quad (6)$$

N_p is the number of atoms in a plane parallel to the surface, T the temperature, $\mu = \mu_A - \mu_B$ the difference of chemical potentials, and Z, Z' the numbers of first neighbors in the same and adjacent planes, respectively.

Minimizing the free energy G with respect to the plane concentrations c_i gives a system of coupled nonlinear equations:[28]

$$\frac{c_i}{1-c_i} = \frac{c}{1-c} \exp\left\{-\frac{\Delta H_i}{kT}\right\}, \quad (7)$$

where c is the bulk concentration, ΔH_i is the segregation enthalpy on the i plane, that is the energy needed to exchange an atom B in the i plane by an atom A from the bulk:

$$\begin{aligned} \Delta H_0 &= \Delta H_0^{\mathrm{size}} + \Delta h_0^{\mathrm{eff}} + V(Z+2Z') - V_0(Z+Z') \\ &\quad + 2Z(V_0 c_0 - Vc) + 2Z'(V_0 c_1 - 2Vc), \\ \Delta H_1 &= \Delta H_1^{\mathrm{size}} + \Delta h_1^{\mathrm{eff}} + VZ' - V_0 Z' + 2ZV(c_1 - c) \\ &\quad + 2Z'(V_0 c_0 + Vc_2 - 2Vc), \\ \Delta H_i &= 2ZV(c_i - c) + 2Z'V(c_{i+1} + c_{i-1} - 2c). \end{aligned} \quad (8)$$

To calculate the equilibrium profile one can use either an area-preserving map algorithm[24,29] or a local field relaxation one.[17,24] In this work we used the second procedure that consists to extract c_i from the left hand side of Eq. (7) and to iterate the system of equations from a set of initial concentrations for a given system size ($N \simeq 20$) and a given bulk concentration determined by imposing the following boundary condition: $c_{N+1} = c$. This procedure converges to a minimum of the free energy. When a first order layering transition occurs (one of the near surface layers going from almost pure B concentration to almost pure A concentration at a given bulk concentration), this procedure gives the stable (absolute minimum of the free energy) and metastable (relative minimum of the free energy) parts of the isotherm. The unstable (maximum of the free energy) part is found using a similar procedure but now fixing the concentration of the layer that undergoes the transition and calculating the remaining concentrations including the bulk one by iteration.

B. Mean-field kinetics

In order to describe the kinetics of either segregation in an A_cB_{1-c} alloy or dissolution of an A deposit into a B substrate we use a simple one-dimensional model consistent with the equilibrium model. This kinetics extension of the TBIM [the KTBIM (Refs. 13 and 22)] also assumes homogeneous concentration per plane parallel to the surface and ensures that the steady state concentration profile corresponds to the equilibrium profile given by Eq. (7). The time dependency of the mean concentration $c_i(t)$ is calculated as a detailed balance between incoming and outcoming fluxes:[30]

$$\frac{\partial c_i}{\partial t} = \frac{D}{d^2}\left[(1-c_i)\left\{\gamma_{i-1}c_{i-1} + \frac{c_{i+1}}{\gamma_i}\right\} - c_i\left\{\frac{(1-c_{i-1})}{\gamma_{i-1}} + \gamma_i(1-c_{i+1})\right\}\right], \tag{9}$$

where $D = D_0 \exp(-Q/kT)$ is the bulk diffusion constant and d the interplanar distance. γ_i represents the transition probability for an exchange between an A atom in plane i and a B atom in plane $i+1$ and it is related to the instantaneous segregation energies:

$$\gamma_i(t) = \exp\left(\frac{\Delta H_i(t) - \Delta H_{i+1}(t)}{2kT}\right). \tag{10}$$

The dynamics of the system is found by iterating the system of Eqs. (9) using a constant time step algorithm. A large number of equations (approximately $N = 5000$) is needed in order to get a dynamics independent of the system size.[31] For the kinetics of segregation we use the initial conditions $c_i(0) = c, i = 0, N$ and the boundary condition $c_{N+1}(t) = c$. For the dissolution kinetics we use $c_0(0) = 1; c_i(0) = 0, i = 1, N$, and $c_{N+1}(t) = 0$.

It is interesting to note that the system of Eqs. (9) is equivalent to the discrete classical Fick's equation when the transition probabilities γ_i tends to 1:

$$\frac{\partial c_i}{\partial t} = \frac{1}{t_0}(c_{i+1} + c_{i-1} - 2c_i), \tag{11}$$

where $t_0 = d^2/D$. This condition can be fulfilled exactly when all the energetic parameters are neglected and approximately when the concentration is weak $c_i \ll 1$.

C. Monte Carlo statics

The Monte Carlo method was also used in conjunction with the energetics provided by the TBIM to study the equilibrium alloy segregation profile and the segregation and dissolution kinetics beyond the mean-field approximation. The calculations were performed in a system box of $l \times l \times m$ fcc unit cells with the largest side (m) oriented along the [111] direction. Periodic boundary conditions were always used in the (111) plane but different boundary conditions were used on the two surfaces along the [111] direction regarding the type of calculation performed.

For equilibrium the standard Metropolis algorithm for Monte Carlo calculations was used.[32] Starting from an arbitrary configuration new system configurations were accepted or rejected according to the thermodynamic probability of their occurrency. The algorithm consists on the repetition of the following steps:

(i) Choose randomly a minority atom.

(ii) Choose randomly another atom in the system box.

(iii) If the second chosen atom is a majority one, calculate the initial $E_{\text{init.}}$ and final (after exchange) E_{final} total energies from Eq. (1).

(iv) Accept the exchange if a random number $r\epsilon(0,1)$ is less than $\exp\{(E_{\text{init.}} - E_{\text{final}})/kT\}$.

Two different types of equilibrium properties were studied at a given temperature T: the bulk solubility limit $c_\alpha(T)$ and the equilibrium segregation profile $c_i(c)$ for bulk concentrations c in the solid solution region of the phase diagram.

In the first case, a closed system of typically $l = 20$, $m = 100$ was used and the initial configuration is formed by 50 contiguous (111) planes of A and 50 B ones. The system is then equilibrated until a $1-c_\alpha/c_\alpha$ interphase is stabilized: c_α is then calculated from the core planes on either side of the interphase. In order to simulate an infinite system, the boundary condition in the [111] direction is imposed by the following procedure: for sites in the top and bottom layers the number of A and B neighbors in the boundary planes outside the systems are computed at random according to tentative bulk concentrations c_{top} and c_{bottom}. For example, a site in the bottom plane (the one in the c_α side of the interphase) has a probability $(1-c_{\text{bottom}})^{Z'}$ to have no neighboring A atoms, a probability $Z'c_{\text{bottom}}(1-c_{\text{bottom}})^{Z'-1}$ to have one neighboring A atom, etc. For consistency the top and bottom tentative concentrations are periodically updated during the simulation to the values of the lately calculated $1-c_\alpha$ and c_α, respectively.

To study the equilibrium segregation profile we also consider a closed system of the same size, but in the [111] direction a free (111) surface is considered in one side while a bottom layer in contact with the bulk and handled as above is taken in the opposite side. For a given number of A atoms the system is set to evolve until thermalization, the surface planes and bulk (arising from the layers close to the bottom side) concentrations are then calculated as temporal averages. Care is taken not to exceed the bulk solubility limit.

D. Monte Carlo kinetics

The kinetics algorithm differs from the equilibrium one because the exchange is performed only between first neighboring atoms. In addition, the study of the Monte Carlo kinetics presents two additional complications: the first one is to impose the boundary condition when the system is allowed to change the number of minority atoms and the second is the more general problem about the definition of the time scale in kinetic Monte Carlo simulations.

Regarding the boundary condition, the number of atoms in the bottom plane is fixed to the corresponding bulk concentration: l^2c in segregation and 0 in dissolution. In the first case, we also calculate the number of A neighbors in the boundary plane below the bottom plane using the same procedure as described for the equilibrium calculations.

In kinetic Monte Carlo simulations "time" is very often measured in "Monte Carlo steps per atom," i.e., the "time" after M attempts is $t(M) = M/N$ where $N = l^2m$ is the total number of sites. If one chooses only minority atoms the "Monte Carlo steps per minority atom" and "Monte Carlo steps per atom" are related by the mean concentration N_A/N where N_A is the number of minority atoms. In our case an additional problem exists due to the nonconstant number of minority atoms during the kinetics. In this case the time in units of "Monte Carlo steps per minority atom" after M attempts is defined by

$$t(M) = \sum_{i=1}^{M} \frac{1}{N_A(i)}, \tag{12}$$

where $N_A(i)$ is the number of minority atoms in the ith attempt.

The initial condition simulates the experimental starting condition: in segregation kinetics we place at random in each plane the number of minority atoms (l^2c) that ensures the homogeneous bulk concentration c. In dissolution we begin with a full surface of A atoms placed over a substrate of B atoms. We typically use a system of lengths $l = 20$ and $m = 1000$ in segregation and dissolution kinetics.

The master equation that describes the kinetics considered above reduces to the 3D random walk equation dynamics in the very dilute case. If one considers now plane averages (f_i) of the site probability, one gets the 1D Fick's equation:

$$\frac{\partial f_i}{\partial \tau} = P_{\text{change}} \frac{Z'}{Z + 2Z'} (f_{i+1} + f_{i-1} - 2f_i), \tag{13}$$

where τ is the Monte Carlo time in units of Monte Carlo steps per minority atom and P_{change} is the probability of accepting an exchange between an atom A and a B one in the very dilute limit, $P_{\text{change}} = 1$ if Metropolis dynamics is used and $P_{\text{change}} = \frac{1}{2}$ if Glauber dynamics[33] is used. The comparison between Eqs. (11) and (13) gives a relation between Monte Carlo time and real time:

$$t = P_{\text{change}} \frac{Z'}{Z + 2Z'} t_0 \tau. \tag{14}$$

This "fortunate" relation is possible thanks to the low solubility limit that enables us to linearize both the KTBIM equations and the Master equation governing the Monte Carlo simulation and also because in this system the kinetics is controlled by bulk diffusion.

For the Ag_cCu_{1-c} system and the (111) face the following values were used[17] for the mentioned energetic quantities: $\Delta H_0^{\text{size}} = -0.25$ eV, $\Delta h_0^{\text{eff}} = -0.11$ eV, $\Delta H_1^{\text{size}} = \Delta h_1^{\text{eff}} = 0$, and $V = -0.032$ eV. Also the prefactor and activation energy for diffusion were taken from Ref. 20: $D_0 = 0.63$ cm^2/s and $Q = 2.02$ eV/atom. Finally, for the (111) orientation, $Z = 6$ and $Z' = 3$.

III. RESULTS

A. Equilibrium surface segregation

The Cu-Ag system is one with a strong tendency to phase separation, as can be seen by the value of the effective pair interaction V calculated from the formation enthalpy $\Delta H = -(Z + 2Z')Vc(1 - c)$. It gives for example a Monte Carlo solubility limit at $T = 1000$ K of $c_\alpha \simeq 0.012$. Regarding the surface segregation in the copper rich region, the three energetic parameters segregate the silver atoms: the negative value of the effective interaction segregates the bulk minority atom, the size effect leads the bigger silver atom to segregate, and the surface tension effect also segregates the Ag atoms due to their lower surface energy. The effect of these three factors is responsible for the layering transitions observed experimentally[14–16] and theoretically[17–19] in this system. Roughly speaking, the inclusion of the effective interaction in the segregation enthalpy ΔH_i gives an i-plane concentration dependency responsible for the phase transition, while the constant terms ΔH_0^{size} and Δh_0^{eff} place the layering transition at a bulk concentration within the solid solution region at this temperature.[34] Using mean-field equations the solubility limit can be found approximately:

$$c_\alpha(T) \simeq \exp\left\{\frac{(Z + 2Z')V}{kT}\right\}, \tag{15}$$

and the critical bulk concentration for the first surface phase transition (the surface concentration going from an almost Cu concentration to an almost Ag concentration) can be also calculated:[19]

$$c_l^0 \simeq \exp\left\{\frac{\Delta H_0^{\text{size}} + \Delta h_0^{\text{eff}} - Z'V_0 + (Z+2Z')V}{kT}\right\} = c_\alpha \exp\left\{\frac{\Delta H_0^{\text{size}} + \Delta h_0^{\text{eff}} - Z'V_0}{kT}\right\}. \quad (16)$$

This first order layering transition occurs if the temperature T is smaller than $T_l^0 = -ZV_0/2k \simeq 1678$ K. A second first order layering transition (the subsurface concentration going from an almost Cu concentration to an almost Ag concentration) occurs at a critical bulk concentration given by

$$c_l^1 \simeq \exp\left\{\frac{Z'V_0 + (Z+Z')V}{kT}\right\} = c_\alpha \exp\left\{\frac{Z'(V_0 - V)}{kT}\right\}, \quad (17)$$

if the temperature is lower than $T_l^1 = -ZV/2k \simeq 1119$ K.

We illustrate this in Fig. 1, where we show the sum of the mean-field surface and subsurface concentrations $c_0 + c_1$ as a function of the bulk concentration c for five different temperatures. As mentioned above at 2000 K ($T > T_l^0 > T_l^1$) the segregation isotherm does not show van der Waal's loop and hence no first order layering transitions are present. At 1500 K and 1200 K, in the temperature region 1119 K $\simeq T_l^1 < T < T_l^0 \simeq 1678$ K, only one van der Waal's loop appears in the lower part of the isotherm corresponding to the surface layering transition. Finally, at 1000 K and 800 K when $T < T_l^1 \simeq 1119$ K, there are two van der Waal's loops, the first one in the lower part of the isotherm that occurs at lower bulk concentration corresponds to the transition of the surface layer and the other one in the higher part of the isotherm and occurring at higher bulk concentration corresponds to the first subsurface layering transition.

In this figure we also show the Monte Carlo results for the same five temperatures. We see a general good agreement between the mean-field and Monte Carlo segregation isotherms, but in Monte Carlo the limiting temperatures T_l^0 and T_l^1 are lower. The new maximum critical temperatures for the first order layering transitions to happen can be estimated taking into account that the maximum critical temperature for the phase separation of a two-dimensional triangular lattice is lower in Monte Carlo than in mean field by a factor of 0.6068;[35] it gives $T_l^0 \simeq 1018$ K and $T_l^1 \simeq 679$ K. It is also interesting to note that the Monte Carlo layering transitions occur at the same bulk concentration than in the mean-field model, suggesting that Eqs. (16) and (17) are also applicables in Monte Carlo. The reason for that is the low bulk concentration that assures that the mean-field approximation is reasonably good.

B. Kinetics of dissolution

Figure 2 shows the dependency of the surface concentration c_0 on the square root of time during the kinetics of dissolution of one Ag monolayer on a Cu substrate at $T = 1000$ K for the mean-field and Monte Carlo models, where the relation between Monte Carlo and mean-field times given by Eq. (14) with $P_{\text{change}} = 1$ (Metropolis dynamics) was used.

There is a remarkable difference between both kinds of descriptions. The mean-field kinetics shows essentially two different regions, the first one with c_0 up to 0.6 being slower and then a speed up of the dissolution. The Monte Carlo kinetics, however, shows a linear behavior, that is a constant dissolution rate in square root of time, that was experimentally observed in this system using Auger spectroscopy.[21]

It shows a clear limitation of the mean-field models that are currently used to study equilibrium and kinetics

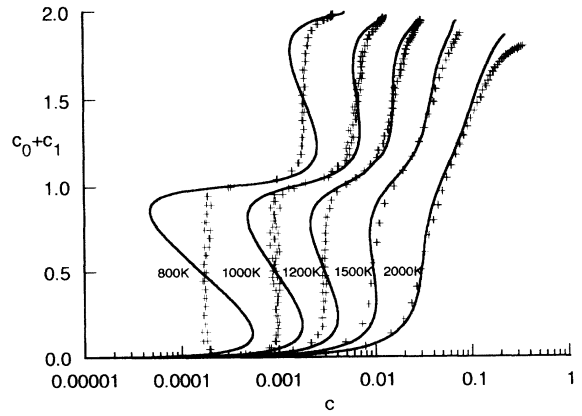

FIG. 1. Mean-field (lines) and Monte Carlo (points) equilibrium segregation isotherms. Sum of the surface c_0 and subsurface c_1 concentrations versus bulk concentration in logarithmic scale at different temperatures.

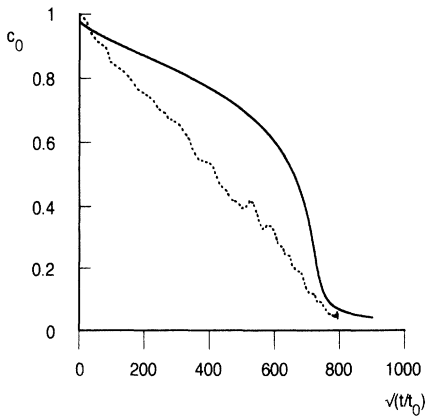

FIG. 2. Dissolution kinetics, c_0 vs $\sqrt{t/t_0}$ at T=1000 K. Comparison between mean field (solid line) and Monte Carlo (dotted line).

of surface segregation even if they have the main energetic ingredients.

A linear growth of the surface concentration with the square root of time is known to happen experimentally during segregation kinetics[36,37] in case of strong segregation. Theoretically it can be found as a solution of the Fick's equation when the subsurface concentration (c_{ss}) is kept constant during the segregation dynamics:

$$c_0(t) = c_0(t=0) + 2(c - c_{ss})\sqrt{\frac{t}{\pi t_0}}, \qquad (18)$$

or in the more complete multilayer models of segregation kinetics when the segregation enthalpy is high.[9,11,31] In the later case the condition of constant subsurface concentration during the kinetics does not need to be imposed artificially because even when $c_{ss}(t)$ is not constant, it remains very small and then its variation in time is also negligible with respect to the bulk concentration c.

The same argument can be used to predict a linear decrease of c_0 with $\sqrt{t}$ if the bulk concentration in Eq. (18) is lower than $c_{ss}(t)$. During dissolution $c = 0$ and then a square root behavior is expected if c_{ss} remains constant.

It makes us pay attention to the subsurface concentrations c_1 and c_2 that are shown in Fig. 3 in function of $\sqrt{t}$. Once again the mean-field and Monte Carlo models show different kinetic behaviors, especially the second subsurface concentration c_2 that is constant in Monte Carlo but shows a time dependency in mean field, explaining the observed difference in $c_0(t)$. It also suggests the identification of c_2 as the subsurface concentration in Eq. (18), the more complicated behavior of c_1 in mean field and its linear decrease in Monte Carlo being related to the companion transition[18,22,38,39] (see below). Using the constant value of $c_2 \simeq 0.001$ as c_{ss} in Eq. (18) and the transformation of Monte Carlo to real time given by Eq. (13) we find the correct slope for the Monte Carlo c_0 versus $\sqrt{t}$ in Fig. 2. In mean field the mentioned slower and faster regions in the c_0 vs $\sqrt{t}$ curve that correspond to c_2 smaller and larger than 0.001, respectively, almost compensate and the total dissolution time for the mean-field kinetics can also be estimated by Eq. (18).

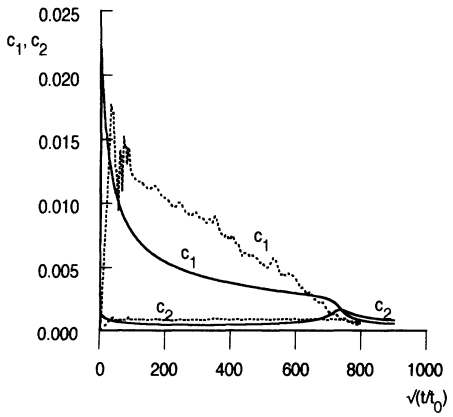

FIG. 3. Dissolution kinetics, c_1 and c_2 vs $\sqrt{t/t_0}$ at T=1000 K. Comparison between mean field (solid lines) and Monte Carlo (dotted lines).

We can understand the different behavior of c_0 and c_2 in Monte Carlo and mean field by means of the local equilibrium concept[13,39,40] that relates the kinetics with the equilibrium surface segregation isotherms.

C. Local equilibrium

As we have already mentioned in Sec. III A there is a strong silver segregation energy that concludes in a high transition probability of exchanging atoms between the surface and subsurface layers. The near surface kinetics is expected to be faster than the bulk kinetics, suggesting that even when the overall profile is far from equilibrium the instantaneous relation between the surface and subsurface concentrations is not different from the one calculated in equilibrium. We can then compare, for example, the relation $c_0(c_2)$ obtained by eliminating the time in $c_0(t)$ and $c_2(t)$ during the kinetics with the relation $c_0(c_2)$ obtained by eliminating the bulk concentration in the equilibrium isotherm $c_0(c)$ and $c_2(c)$.

In Fig. 4(b), we show this comparison at T = 1000 K

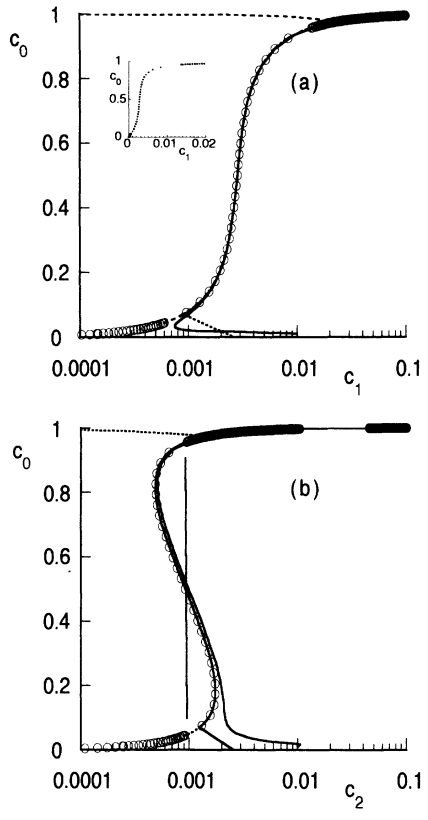

FIG. 4. Mean-field local equilibrium at T=1000 K, (a) c_0 vs c_1 and (b) c_0 vs c_2 (see the horizontal logarithmic scale). Segregation at c=1% (solid line), segregation at c=0.25% (dotted line), dissolution (dashed line), and equilibrium (circles). The inset in (a) shows the equilibrium c_0 vs c_1 in a linear horizontal scale and the vertical line in (b) shows the position of the first order transition found using the Monte Carlo model.

using the mean-field model: the equilibrium isotherm shows the first order transition mentioned in Sec. III A. As suggested, during the dissolution the $c_0(c_2)$ curve follows the equilibrium one, including the metastable and unstable parts of the equilibrium isotherm. Taken into account that c_0 is monotonous with $\sqrt{t}$ it is easy to recognize in Fig. 3 the van der Waal's loop that causes c_2 to have two relative maxima and one minimum as a function of $\sqrt{t}$.

Figure 5(b) shows the local equilibrium now using the Monte Carlo model. The first order transition is also present but without a van der Waal's loop. The transition happens at the same value (in c_2) than in the mean-field calculation as we have marked in Fig. 4(b). We see that now also during the dissolution the $c_0(c_2)$ curve follows the equilibrium one and the absence of van der Waal's loop in this case explains the constant value of c_2 seen in Fig. 3.

A similar procedure can be done in order to correlate the surface c_0 and first subsurface c_1 concentration that we show in Figs. 4(a) and 5(a) for the mean-field and Monte Carlo cases, respectively. The local equilibrium concept is also well verified but the equilibrium isotherm is slightly more complicated due to the existence of a companion transition. It is a small jump of c_1 (from 0.0006 to 0.014 in mean field) when c_0 undergoes its first order transition. The mean field c_0 vs c_1 curve is then the composition of two van der Waal's loops that has the effect to finally get a monotonous but not simple c_0 vs c_1 curve. The kinetic behavior of c_1 presented in Fig. 3 is the consequence of that. In Monte Carlo there also exists the companion transition but no van der Waal's loop is present. In this case c_0 growths linearly with c_1 inside the transition [see the inset of Fig. 5(a)], which is consistent with the linear decrease of c_1 with $\sqrt{t}$ in Fig. 3.

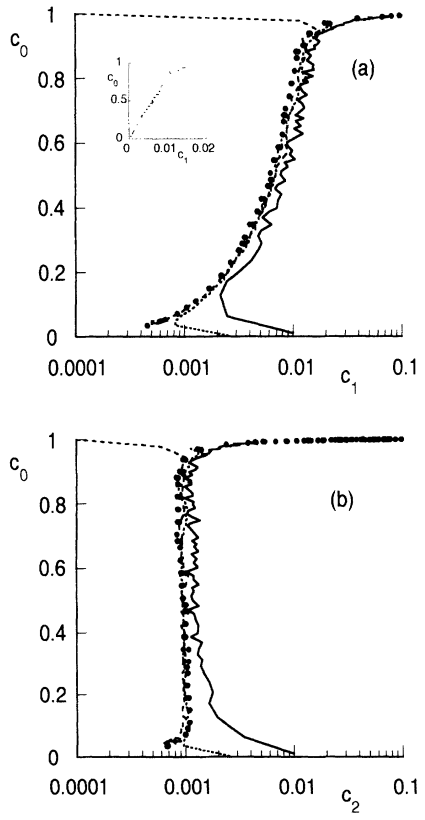

FIG. 5. Monte Carlo local equilibrium at T=1000 K, (a) c_0 vs c_1 and (b) c_0 vs c_2 (see the horizontal logarithmic scale). Segregation at c=1% (solid line), segregation at c=0.25% (dotted line), dissolution (dashed line), and equilibrium (points). The inset in (a) shows the equilibrium c_0 vs c_1 in a linear horizontal scale.

D. Kinetics of surface segregation

Figure 6 shows the kinetics of segregation at $c = 1\%$ and $T = 1000$ K for the mean-field and Monte Carlo kinetics. We have found in this case that both models show an almost linear dependency in $\sqrt{t}$ slightly more exact in Monte Carlo than in mean field. It also agrees with the experimental observation in Cu-Ag for the (111) surface.[21] As mentioned in Sec. III B this behavior is related with the existence of a constant subsurface concentration and then a constant $c_2(t)$ is expected during the increase of c_0.

Figure 7 shows the first and second subsurface concentrations. After the initial fast transient regime we see that the Monte Carlo c_2 presents a small drift to lower values until $\sqrt{t/t_0} \simeq 50$ and the mean field c_2 shows a slightly bigger drift now up to $\sqrt{t/t_0} \simeq 100$. However, in both cases the variation of the second subsurface concentration $\Delta c_2 \simeq 0.0015$ is small when compared to the bulk concentration $c = 0.01$.

We can wonder if the local equilibrium is also satisfied in this case. Figure 4(b) shows that this is the case when the mean-field model is used. It also explains the drift observed in Fig. 7 since c_2 shows a monotonous decrease while c_0 grows up to 0.8 due to the van der Waal's loop. In Monte Carlo the local equilibrium is also well verified as shown in Fig. 5(b). The decrease of c_2 while c_0 increases up to 0.4 suggests a slower approach to the

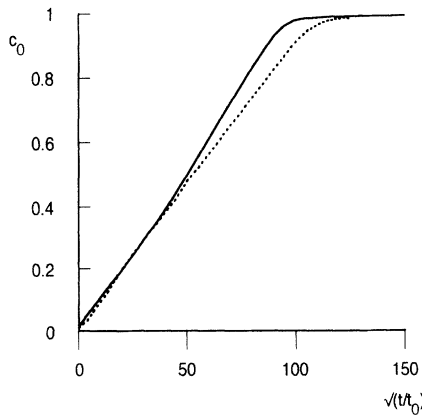

FIG. 6. Segregation kinetics, c_0 vs $\sqrt{t/t_0}$ at T=1000 K and c=1%. Comparison between mean field (solid line) and Monte Carlo (dotted line).

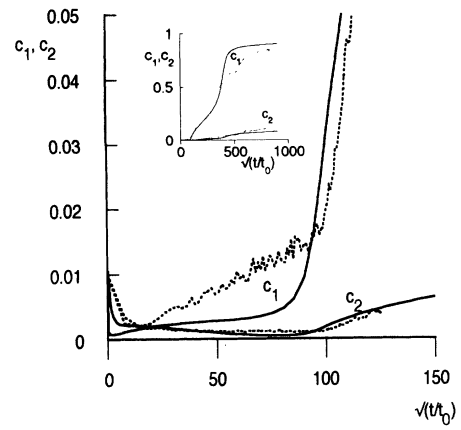

FIG. 7. Segregation kinetics, c_1 and c_2 vs $\sqrt{t/t_0}$ at T=1000 K and c=1%. Comparison between mean field (solid lines) and Monte Carlo (dotted lines). The inset shows a larger time scale.

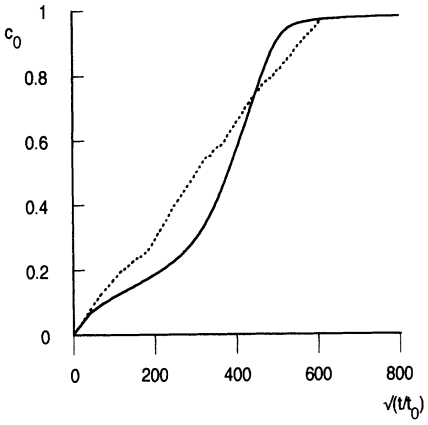

FIG. 9. Segregation kinetics, c_0 vs $\sqrt{t/t_0}$ at T=1000 K and c=0.25%. Comparison between mean field (solid line) and Monte Carlo (dotted line).

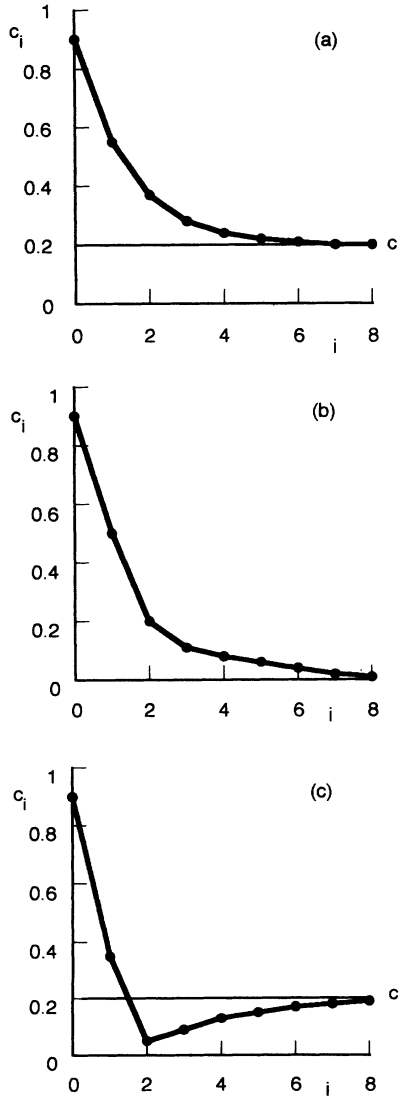

FIG. 8. Schematic concentration profile in (a) equilibrium, (b) dissolution kinetics, and (c) segregation kinetics.

equilibrium isotherm during segregation kinetics than in dissolution.

The local equilibrium is better verified in dissolution than in segregation also when the mean field model is used (see Fig. 4). It can be understood by comparing the schematic concentration profiles in equilibrium, and during dissolution and segregation kinetics, that we show in Fig. 8. The equilibrium profile is a monotonous decreasing function with respect to the surface distance and the same behavior is expected for the instantaneous profile during dissolution in order to have a net flux going into the bulk. In segregation kinetics, not only the instantaneous profile is not monotonous but also as the flux is directed to the surface an increasing profile in function of the surface distance is expected beginning at the second subsurface layer.

A mean-field and Monte Carlo difference similar to the one seen during dissolution can also be illustrated in segregation by choosing a smaller bulk concentration in order to make relevant the variation of c_2 with respect to c. Figure 9 shows the surface concentration during segregation kinetics at c = 0.0025; it increases linearly in $\sqrt{t}$ in Monte Carlo but not in mean field. In Fig. 10

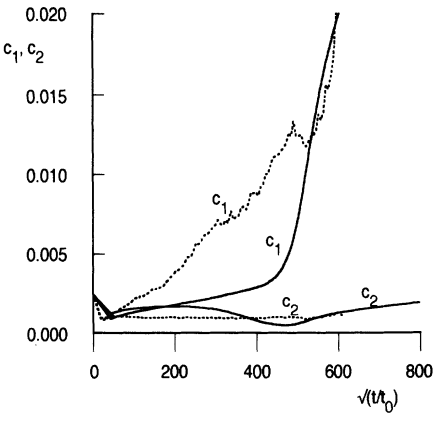

FIG. 10. Segregation kinetics, c_1 and c_2 vs $\sqrt{t/t_0}$ at T=1000 K and c=0.25%. Comparison between mean field (solid lines) and Monte Carlo (dotted lines).

we see that this difference is correlated to the invariance of the second subsurface concentration in the first case and the bigger variation of c_2 relative to c in the second one. Figures 4 and 5 show that the local equilibrium is once again satisfied. Also the lower the bulk concentration, the slower the kinetics and in consequence the local equilibrium is even better satisfied.

The linear dependency of the Monte Carlo c_1 in $\sqrt{t}$ that can be seen after the initial transient and during the linear increase of c_0 in Figs. 7 and 10 is also a consequence of the local equilibrium and the linear dependence between c_0 and c_1 inside the transition due to the already mentioned companion transition. The inset in Fig. 7 shows the way c_1 reaches the equilibrium. We see in Fig. 1 that at $c = 1\%$ and $T = 1000$ K the equilibrium c_1 is very close to 1 and that there is also a first order layering transition involving c_1 in mean field but not in Monte Carlo. However, there is no linear dependency of c_1 on the square root of time: in both cases because the variation of c_3 while c_1 growths is comparable to the bulk concentration c. At $c = 0.25\%$ the equilibrium c_1 is close to 0.05, no first order transitions happens and the segregation equilibrium is slowly reached.

IV. DISCUSSION AND CONCLUSION

In this paper, we have studied the kinetics of segregation in Cu-Ag alloys and the kinetics of dissolution of one Ag monolayer deposited on Cu(111). We find that using the kinetic Monte Carlo model the experimental square root dependency with time of the surface concentration is found for the segregation and dissolution kinetics. We have also shown that the homogeneous mean-field calculations cannot take into account correctly these phenomena: the surface concentration during the kinetics of segregation and dissolution cannot present the experimentally observed square root dependency on time. The reason is that during the mean-field kinetics the second subsurface concentration follows a van der Waal's loop in function of time instead of remaining constant as in Monte Carlo. However, the importance of this variation in c_2 in segregation kinetics is relatively diminished at higher bulk concentration (when $\Delta c_2 \ll c - c_2$) but in dissolution kinetics it is never the case because the bulk concentration is zero and $\Delta c_2 \simeq c_2$.

The local equilibrium concept allowed us to understand that the constant value of c_2 in Monte Carlo corresponds to the one at which a first order layering transition occurs. During the segregation and dissolution kinetics the surface concentration c_0 drops into the surface phase separation region ($0.05 < c_0 < 0.95$) and regions of high and low surface concentrations are expected. It suggests that a rich behavior of island growth or coarsening can be expected as a consequence of the first order transition. Figure 11 shows a snapshot of the surface microstructure at the end of the dissolution kinetics ($c_0 \simeq 0.2$) and $T = 1000$ K. Isolated silver atoms and islands are both present representing the low and high surface concentration phases. The presence of Ag islands has been recently observed experimentally by Auger line scans during the transition.[15] One can wonder what is the local environment of the surface atoms that preferentially enter into the bulk. Energetically isolated atoms have *a priori* a bigger probability to enter than island border atoms and the last ones a bigger probability than the ones at the island center. Calculations to quantify this effect and its relation with island growth or coarsening are currently in progress.

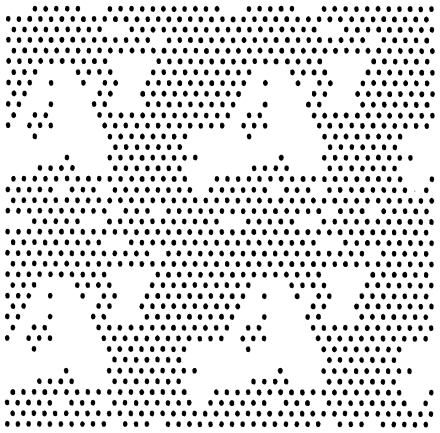

FIG. 11. Snapshot of the surface microstructure during Monte Carlo dissolution kinetics at T=1000 K. White points represent Ag atoms and black points represent Cu atoms. For sake of clarity four surface cells are shown.

ACKNOWLEDGMENTS

We wish to acknowledge fruitful discussion with J. Eugène, B. Aufray, and P. Bellon. One of us (A.S.) also acknowledges helpful correspondence with E. Werthein.

[1] A. R. Miedema, Z. Metallk. **69**, 455 (1978).
[2] J. R. Chelikowsky, Surf. Sci. **139**, L197 (1984).
[3] S. Mukherjee and J. L. Morán López, Surf. Sci. **188**, L742 (1987).
[4] P. M. Ossi, Surf. Sci. **201**, L519 (1988).
[5] G. Tréglia, B. Legrand, and F. Ducastelle, Europhys. Lett. **7**, 575 (1988).
[6] P. J. Schmitz, W. Y. Leung, G. W. Graham, and P. A. Thiel, Phys. Rev. B **40**, 11 477 (1989).
[7] C. T. Chan, K. P. Bohnen, and K. M. Ho, Phys. Rev. Lett. **69**, 1672 (1992).
[8] S. Rousset, S. Chiang, D. E. Fowler, and D. D. Chambliss,

Phys. Rev. Lett. **69**, 3200 (1992).
[9] S. Hofmann and J. Erlewein, Surf. Sci. **77**, 591 (1978).
[10] S. Kristyan and J. Giber, Surf. Sci. **224**, 476 (1989).
[11] J. du Plessis and P.E. Viljoen, Surf. Sci. **276**, L7 (1992).
[12] Cs. Cserháti, H. Bakker, and D. L. Beke, Surf. Sci. **290**, 345 (1993).
[13] A. Senhaji, G. Tréglia, B. Legrand, N. T. Barrett, C. Guillot, and B. Villette, Surf. Sci. **274**, 297 (1992).
[14] Y. Liu and P. Wynblatt, Surf. Sci. Lett. **241**, L21 (1991).
[15] Y. Liu and P. Wynblatt, Surf. Sci. **290**, 335 (1993).
[16] J. Eugène, B. Aufray, and F. Cabané, Surf. Sci. **241**, 1 (1991).
[17] G. Tréglia, B. Legrand, J. Eugène, B. Aufray, and F. Cabané, Phys. Rev. B **44**, 5842 (1991).
[18] Y. Liu and P. Wynblatt, Surf. Sci. Lett. **240**, 245 (1990).
[19] J. Eugène, G. Tréglia, B. Legrand, B. Aufray, and F. Cabané, Surf. Sci. **251**, 664 (1991).
[20] J. Eugène, B. Aufray, and F. Cabané, Surf. Sci. **273**, 372 (1992).
[21] J. Eugène, Ph.D. thesis, Université d'Aix Marseille III, 1989; H. Giordano, Ph.D. thesis, Université d'Aix Marseille III, 1993; and B. Aufray (private communication).
[22] A. Senhaji, G. Tréglia, J. Eugène, A. Khoutami, and B. Legrand, Surf. Sci. **287/288**, 371 (1993).
[23] A. Saúl, B. Legrand, and G. Tréglia, Surf. Sci. **307/309**, 804 (1994).
[24] F. Ducastelle, B. Legrand, and G. Tréglia, Prog. Theor. Phys. Suppl. **101**, 159 (1990).
[25] F. Ducastelle and F. Gautier, J. Phys. F **6**, 2039 (1976).
[26] D. Tománek, A. A. Aligia, and C. A. Balseiro, Phys. Rev. B **32**, 5051 (1985).
[27] V. Rosato, M. Guillopé, and B. Legrand, Philos. Mag. A **59**, 321 (1989).
[28] G. Tréglia and B. Legrand, Phys. Rev. B **35**, 4338 (1987).
[29] R. Pandit and M. Wortis, Phys. Rev. B **25**, 3226 (1986).
[30] G. Martin, Phys. Rev. B **41**, 2279 (1990).
[31] A. Saúl, B. Legrand, G. Tréglia, J. Eugène, B. Aufray, and H. Giordano (unpublished).
[32] N. Metropolis, A. W. Metropolis, M. N. Rosenbluth, A. H. Teller, and E. Teller, J. Chem. Phys. **21**, 1087 (1953).
[33] R. J. Glauber, J. Math. Phys. **4**, 294 (1963).
[34] C. R. Helms, Surf. Sci. **69**, 689 (1977).
[35] See, for example, M. E. Fisher, Rep. Prog. Phys. **30**, 615 (1967).
[36] J. du Plessis, Solid State Phenom. **11**, 1 (1990).
[37] J. du Plessis and P. E. Viljoen, Surf. Sci. **131**, 321 (1983).
[38] Y. Teraoka and T. Seto, Surf. Sci. **255**, 209 (1991).
[39] A. Saúl, B. Legrand, and G. Tréglia, in *Materials Science Forum*, edited by Y. Limoge and J. L. Boquet (Trans. Tech., Switzerland, in press).
[40] M. Lagües and J. L. Domange, Surf. Sci. **47**, 77 (1975).

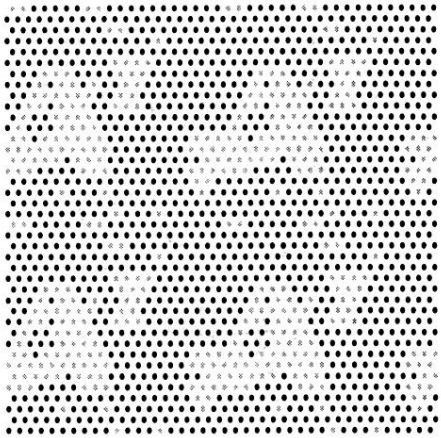

FIG. 11. Snapshot of the surface microstructure during Monte Carlo dissolution kinetics at T=1000 K. White points represent Ag atoms and black points represent Cu atoms. For sake of clarity four surface cells are shown.